Mineralogy and Petrology (2018) 112:801–817
https://doi.org/10.1007/s00710-018-0597-4

ORIGINAL PAPER

Petrogenesis of ore-bearing porphyry in non-subduction setting: a case study of the Eocene potassic intrusions in the western Yangtze Block

Zheng Liu[1,2] · Shi-Yong Liao[3] · Qing Zhou[4] · Xin Zhang[2]

Received: 6 December 2017 / Accepted: 21 May 2018 / Published online: 29 May 2018

Abstract
In the western Yangtze Block, abundant Eocene (~38–34 Ma) potassic adakite-like intrusions and associated porphyry copper deposits are exposed in non-subduction setting, including Machangjing, Beiya, Binchuan, Habo and Tongchang intrusions. All these ore-bearing porphyries share many geochemical characteristics of adakite such as depletion in heavy rare earth elements (HREEs), enrichment in Sr and Ba, absence of negative Eu anomalies, high SiO_2, Al_2O_3, Sr/Y, La/Yb and low Y, Yb contents. They also exhibit affinities of potassic rocks, e.g., alkali-rich, high K_2O/Na_2O ratios and enrichment in light rare earth elements (LREEs) and large ion lithophile elements (LILEs). Their Sr-Nd isotopic ratios are similar to coeval shoshonitic lamprophyres. Geochemical data indicate that they were probably produced by partial melting of newly underplated potassic rocks sourced from a modified and enriched lithospheric mantle. These underplated rocks have elevated oxygen fugacity, water and copper contents, with high metallogenic potential. We propose that all the studied potassic rocks were emplaced in a post-collisional setting, associated with the local removal of lithospheric mantle.

Keywords Potassic rocks · Lithospheric mantle · Porphyry copper deposit · Eocene · Western Yangtze

Introduction

Adakite represents a group of intermediate-felsic igneous rocks that are emplaced in modern arc systems. Adakite is notably characterized by its enrichment in high Al_2O_3 (> 15 wt.%), low Y (≤ 18 ppm) and Yb (≤ 1.9 ppm), as well as its high Sr/Y (> 20–40) and La/Yb (> 20) ratios with positive Sr and Eu anomalies (e.g. Defant and Drummond 1990, 1993; Castillo et al. 1999; Defant and Kepezhinskas 2001; Moyen 2011). These rocks have been interpreted to be derived by the interaction of melts derived from hot and young subducted slab with the overlying mantle wedge during ascent (Defant and Drummond 1990). It should be pointed out that the term "adakite", including "C-type adakite", "continental adakite" and "potassic adaktie" (e.g., Rapp et al. 2002; Wang et al. 2004a, b, 2006; Guo et al. 2006; Ding et al. 2007; Li et al. 2013), has been used in a more ambiguous manner in several subsequent studies. These phrases in reality refer to the intermediate to acid igneous rocks with high La/Yb (> 20), high Sr (> 400 ppm) and low Y (< 18 ppm), Yb (< 1.9 ppm) contents, which are regarded as "adakite-like" or "adakitic" geochemical signatures (Moyen 2009). Therefore, in our current study, the term "adakite" is used to describe rocks sourced from subducted slab, whereas "adakitic" or "adakite-like" rocks refer to those having different sources. Several hypotheses have been proposed for the formation of adakite-like rocks, such as (1) direct partial melting of a metasomatized lithospheric mantle (e.g. Martin et al. 2005; Jiang et al. 2006, 2012); (2) high- or low-pressure assimilation-fractional crystallization (AFC) of mantle-derived mafic magmas (Castillo et al. 1999; Richards and Kerrich 2007); (3) partial melting of

Editorial handling: X. Xu

✉ Zheng Liu
zhengliu@lzu.edu.cn

[1] School of Resource Environment and Earth Science, Yunnan University, NO. 2 Cuihuabei Road, Kunming, Yunan 650091, People's Republic of China

[2] School of Earth Sciences, Gansu Key Laboratory of Mineral Resources in Western China, Lanzhou University, Lanzhou 730000, People's Republic of China

[3] Key Laboratory of Planetary Sciences, Purple Mountain Observatory, Chinese Academy of Sciences, Nanjing 210008, People's Republic of China

[4] Chengdu Institute of Geology and Mineral Resources, Chengdu 610081, People's Republic of China

delaminated eclogitic lower crust (e.g. Xu et al. 2002); (4) partial melting of thickened lower crust (e.g. Hou et al. 2004).

Porphyry Cu deposits constitute a significant source of Cu, Mo and Au (Sillitoe 2010). It is well established that these deposits were closely associated with adakites in arc setting (e.g., Thieblemont et al. 1997; Richards 2011a, b). This geological relationship is supported by observations on different scales: (1) on a global scale, adakitic igneous provinces generally overprint porphyry Cu metallogenic belts; (2) on a district scale, porphyry and epithermal mineral deposits are often hosted by or associated with adakties; (3) on a deposit scale, the mineralization prefers adakites to other igneous rocks (Thieblemont et al. 1997). Recently, porphyry Cu systems occurring in adakite-like rocks have been also reported (Hou

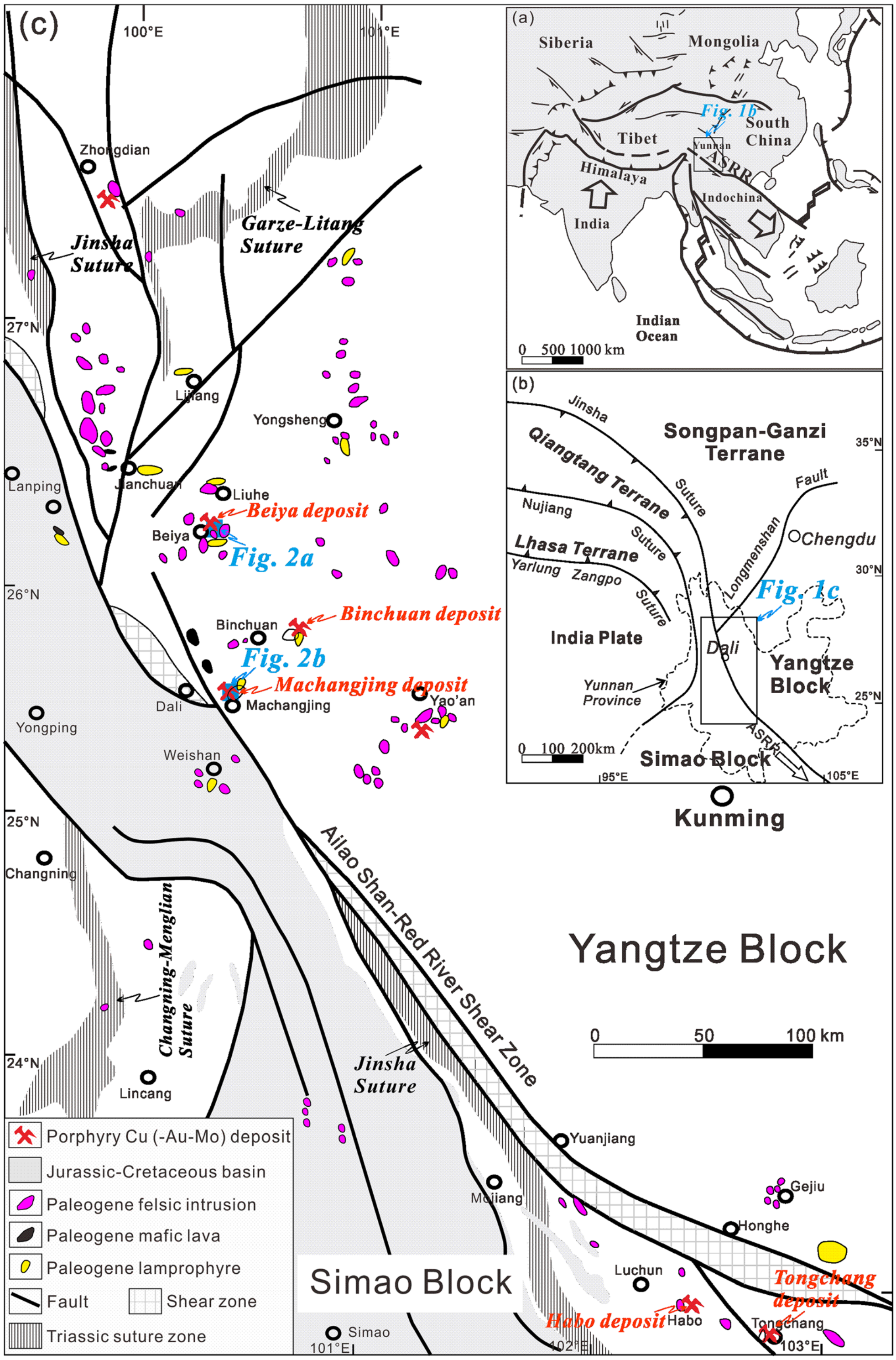

Fig. 1 **a** Major Cenozoic fault systems in Asia (Tapponnier et al. 1990); **b** Tectonic framework of the eastern Tibet (Lu et al. 2015a); **c** Simplified geological map of the southeastern Tibetan plateau and surrounding areas showing the distribution of Cenozoic potassic igneous rocks in western Yangtze (modified after Lu et al. 2013a, 2015a)

et al. 2009; Richards 2011a, b; Lu et al. 2013b), such as the mid-Miocene Gangdese and Eocene-Oligocene Yulong porphyry Cu (-Mo) belts in the Himalayan orogenic belt (Hou et al. 2003, 2009; Jiang et al. 2006). These belts were formed in non-subduction setting (an intracontinental convergent environment) in response to the Himalayan-Tibetan collisional orogeny (Hou et al. 2003). However, the link between porphyry Cu deposit and ore-bearing porphyries in non-subduction settings remains poorly understood.

In the western Yangtze Block (western Yunnan province), porphyry Cu deposits are hosted by Eocene-Oligocene post-collisional adakite-like intrusions in response to the Indo-Asian collision (Fig. 1a). These intrusions provide an excellent opportunity for researchers to better understand the geodynamic processes that drive the generation of post-collisional ore-bearing porphyries. In this paper, we investigate multiple Eocene ore-bearing porphyries and coeval lamprophyric dykes in Western Yunnan (Fig. 1b). New whole-rock major, trace elemental and Sr–Nd isotopic data for these intrusions are presented in this paper. Previous reported data on coeval lamprophyres and other ore-bearing porphyries are also included for comparison. Our major goals are to better understand (i) the origin of these rocks; (ii) their geological relationship with porphyry copper deposits, and (iii) the associated geodynamic processes.

Geological background

The current study focused in a junction zone on western Yunnan province between the Simao (the northern part of Indochina Block; Metcalfe 2013) and Yangtze Block, where the ASRR shear zone locally overprints the Jinsha suture (Guo et al. 2005; Lu et al. 2012, 2013a, b) (Fig. 1c). The Yangtze Block has an Archaean-Proterozoic basement composed of high-grade metamorphic and metasedimentary rocks (Gao et al. 1999), whereas the Precambrian metamorphic rocks of the Simao block include Proterozoic migmatite, granulite and schist (Wang et al. 2014). The collision between the two blocks occurred during the Triassic and resulted in the closure of the Paleozoic Jinsha Ocean (Yang 1998; Wang et al. 2000). Since Triassic, *W. Yunnan* has occupied an intra-continental position (Wang et al. 2000; Lu et al. 2015a).

In the Cenozoic, the India Plate collided with the Asian Plate and subsequently extruded the Indochina Block with emplacement of extensive Palaeocene potassic mafic and felsic rocks (Fig. 1c). The mafic rocks are dominated by lamprophyric dykes with minor mafic lavas, whereas the felsic rocks are mainly composed of syenite porphyry, quartz monzonite porphyry and monzogranite porphyry. These mafic and felsic intrusions intruded predominant non-metamorphosed sedimentary sequences (Liang et al. 2007; Lu et al. 2012, 2013a). The felsic rocks exhibit many geochemical characteristics of typical adakites (Lu et al. 2013a) and contain porphyry Cu (-Au-Mo) deposits (Deng et al. 2014), including Beiya Cu–Au ore field, Binchuan Cu deposit, Machangjing Cu–Mo–Au deposit, Habo Cu–Au ore deposit and Tongchang Cu–Mo deposit along with others (Deng et al. 2014; Fig. 1c). Abundant crustal and mantle xenoliths are present in these felsic intrusions, especially in the Liuhe syenite porphyry (Fig. 1c). The xenoliths include garnet-bearing amphibolite from the middle crust (~ 30 km

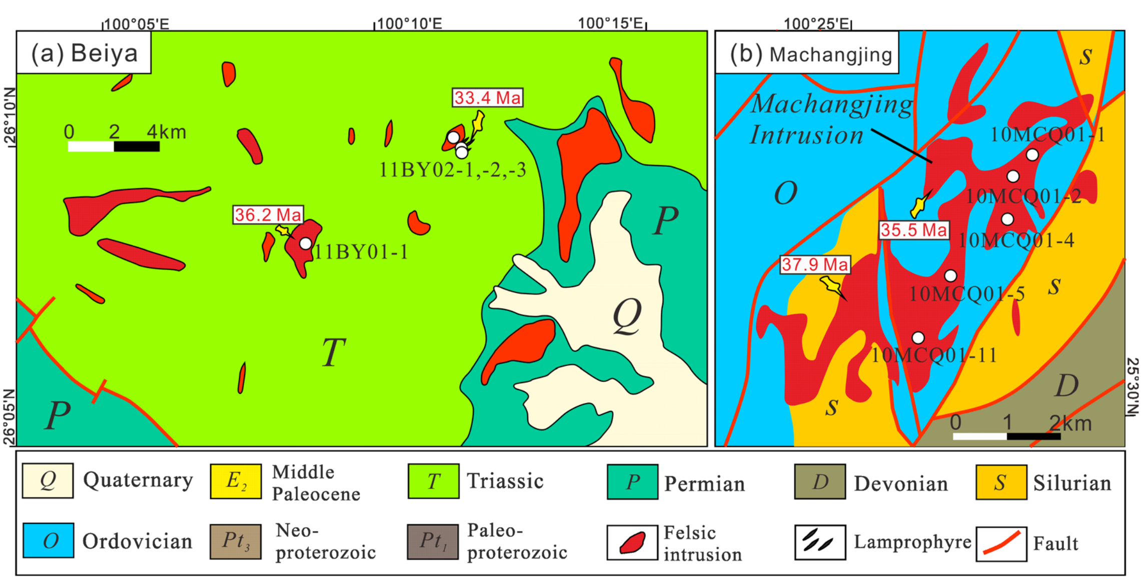

Fig. 2 Simplified geological maps of the investigated intrusions, including the Beiya (**a**) and Machangjing (**b**) intrusions. Ages of these felsic intrusions and lamprophyres are also exhibited and the data sources are same as Table 1

depth), granulite from the lower crust (~ 45–55 km depth) and garnet pyroxenite from the upper mantle (~87–95 km depth) (Zhao et al. 2003).

Petrography

In this contribution, we collected samples from potassic intrusions and lamprophyre dykes at Beiya and Machangjing. The Beiya intrusion, which occurs as a group of felsic stocks, were emplaced in Triassic-Permain volcanics and limestone (Fig. 2a). It consists of syenite porphyry and granite porphyry with typical porphyritic texture (Table 1). The main constituents of the phenocrysts (1–4 mm, ~ 40–60%) are K-feldspar, plagioclase and biotite, with hornblende and quartz as minor components. The groundmass (50–60%) exhibits a microcrystalline texture and is composed mainly of K-feldspar and plagioclase, with a small amount of quartz. Some lamprophyric dykes from the Beiya region intruded Triassic strata (Fig. 2a). These lamprophyres are porphyritic with phenocrysts (1–2 mm, 40%), dominated by clinopyroxene, hornblende and phlogopite in a groundmass of clinopyroxene-hornblende-phlogopite-plagioclase. The Machangjing intrusion consists of syenite porphyry and granite porphyry with a typical porphyritic texture (Table 1) and was emplaced in Ordovician-Devonian sandstone and limestone (Fig. 2b). The phenocrysts (1–3 mm, ~ 30–40%) are constituted of K-feldspar, plagioclase, biotite and quartz. The groundmass (60–70%) is composed of K-feldspar, plagioclase and biotite with a microcrystalline texture. Also, previous data on the coeval lamprophyres and ore-bearing Beiya, Binchuan, Habo and Tongchang porphyries are also summarized in this paper for comparison. These intrusions consist primarily of syenite porphyry, quartz monzonite porphyry and granite porphyry. The detailed texture and mineralogy for them are summarized in Table 1. Previous studies implied that all the studied lamprophyre dykes and porphyry intrusions were formed in the Eocene with magmatic crystallization ages of ~38–34 Ma (Table 1).

Sample descriptions and analytical methods

Sampling

We collected samples (length: 20 to 30 cm, width: 15 to 20 cm, height: 10 to 20 cm) from surface exposures and prospecting trench. They are representative due to come from both edges and centers of the studied intrusions. The freshest nine samples, including two samples (11BY01–1, 11BY02–1) from the Beiya intrusion, two samples (11BY02–2, 11BY02–3) from the Beiya lamprophyres and five samples (10MCQ01–1 ~ −5) from the Machangjing intrusion, were selected for the analysis of whole-rock major and trace

Table 1 Zircon ages and characteristics of investigated intrusions and lamprophyres

Intrusion	Rock type	Texture	Mineralogy	Accessory minerals	Age (Ma)	±	Method	Reference
Beiya	Syenite porphyry/granite porphyry	Porphyritic, microcrystalline for groundmass	Phenocrysts: Kfs + Pl ± Bt ± Hbl ± Qz; Groundmass: Kfs + Pl + Qz	Ap + Ttn + Mag + Zrn	36.2	0.6	LA-ICP-MS	He et al. (2012)
	Lamprophyre	Lamprophyric texture	Phenocrysts: Cpx + Hbl + Phl; Groundmass:Cpx + Hbl + Phl + Pl	Ap + Mag	33.4	0.6	$^{40}Ar/^{39}Ar$	Xue et al. (2008)
Machangjing	Granite porphyry	Porphyritic, microcrystalline for groundmass	Phenocrysts: Kfs + Pl + Qz + Bt; Groundmass: Kfs + Pl + Bt	Ap + Ttn + Zrn ± Mag	37.9	0.8	LA-ICP-MS	He et al. (2011)
	Syenite porphyry	Porphyritic, microcrystalline for groundmass	Phenocrysts: Kfs; Groundmass: Kfs + Pl + Bt	Ap + Ttn + Zrn	35.5	0.4	K-Ar	Peng et al. (2005)
Binchuan	Granite porphyry	Porphyritic, microcrystalline for groundmass	Phenocrysts: Kfs + Pl + Qz + Bi; Groundmass: Kfs + Pl + Qtz	Ap + Zrn	35	0.1	LA-ICP-MS	Xu et al. (2015)
Habo	Quartz monzonite porphyry	Porphyritic, microcrystalline for groundmass	Phenocrysts: Kfs + Pl + Qz + Bi+Hbl; Groundmass: Kfs + Pl ± Qz	Ap + Ttn + Zrn ± Mag	36.2	0.2	LA-ICP-MS	Zhu et al. (2013)
	Granite porphyry	Porphyritic, microcrystalline for groundmass	Phenocrysts: Kfs + Pl + Qz + Bt; Groundmass: Kfs + Pl + Bt	Ap + Ttn + Zrn ± Mag	35.4	0.5	LA-ICP-MS	Zhu et al. (2013)
Tongchang	Quartz syenite porphyry	Porphyritic, microcrystalline for groundmass	Phenocrysts: Kfs + Pl + Qz + Hbl; Groundmass: Kfs + Pl + Qz	Ap + Ttn + Zrn	34.5	0.4	LA-ICP-MS	Liang et al. (2007)

Mineral abbreviations: *Kfs* K-feldspar, *Qz* quartz, *Cpx* clinopyroxene, *Bt* biotite, *Pl* plagioclase, *Hbl* hornblende, *Mag* magnetite, *Ap* apatite, *Ttn* titanite, *Zrn* zircon (Whitney and Evans 2010) elements as well as Sr-Nd isotopes. The sample locations are shown in Fig. 2. These samples are first crushed to gravel-size chips and then further grounder to less than 200-mesh in an agate mill prior to the whole-rock analyses.

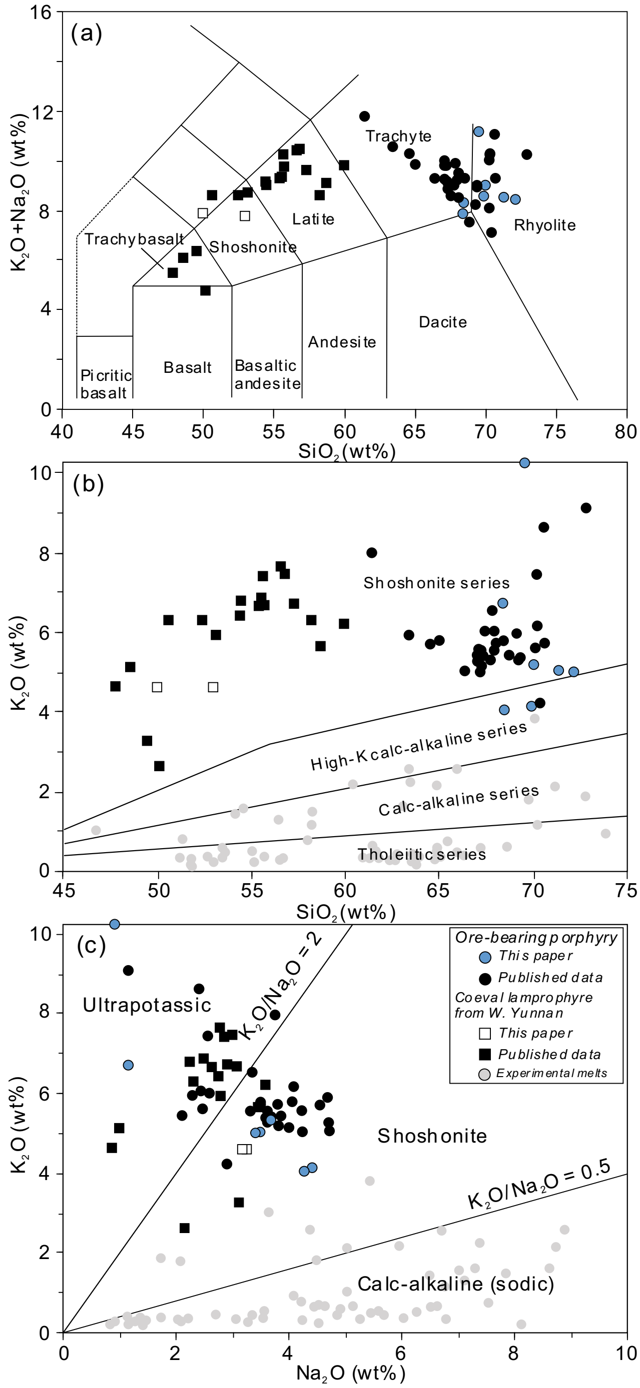

Fig. 3 **a** TAS diagram (Le Maitre 2002), (**b**) K_2O vs. SiO_2 diagram (Peccerillo and Taylor 1976) and (**c**) Na_2O vs. K_2O diagram of the lamprophyres and ore-bearing intrusions; previous data concerning the coeval lamprophyres (Li et al. 2002; Lu et al. 2015a), Beiya (Xu et al. 2006; Lu et al. 2013a), Tongchang (Xu et al. 2011; Tran et al. 2014), Binchuan (Lu et al. 2013a) and Habo (Zhu et al. 2013) intrusions are also shown for comparison; Only those least altered samples (LOI < 1.5) are plotted in the diagram. Data of amphibolite experimental melts are also exhibited. Data sources: Sen and Dunn (1994) and Rapp and Watson (1995)

Major and trace elements

The major elements in the samples were identified by X-ray fluorescence (XRF) using fused glass beads on a Rigaku ZSX100e spectrometer (Rigaku, Tokyo, Japan) at the Analytical Center, Chengdu Institute of Geology and Mineral Resources. Analysis of the international rock standard (GSR-1 and GSR-3) suggests than both precision and accuracy are better than 5% of error.

For analyzing the abundances of trace element, 50 mg of each grounded sample was dissolved at about 190 °C for 48 h in a Teflon bomb containing a mixture of 1.5 mL HNO_3 and 1.5 mL HF. Subsequently, the bomb was opened to allow complete evaporation of the solution at about 115 °C until it is dry. This process is followed by addition of 1 ml HNO_3. After the solution was evaporated to dryness again, 3 mL of 30% HNO_3 was added to re-dissolve the precipitates. The bomb was then resealed and reconstituted solution inside was heated to 190 °C for 12 to 20 h before being diluted by 2% HNO_3 to 100 g by for analysis. The abundances of trace

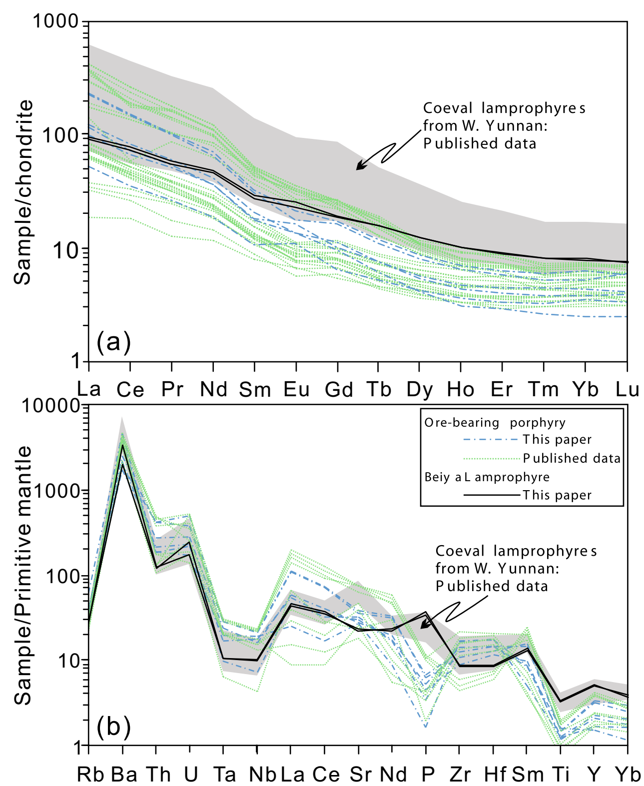

Fig. 4 Chondrite-normalized (Boynton 1984) REE patterns (a) and primitive mantle-normalized (McDonough and Sun 1985) trace element patterns (b) for the felsic intrusions and coeval lamprophyres. Additional data sources are same as Fig. 3

elements were determined on an Agilent 7500a Inductively Coupled Plasmas-Mass Spectrometry (ICP-MS) at the State Key Laboratory of Geological Processes and Mineral Resources, China University of Geosciences Wuhan (SKLGPMR, CUGW). Analyses of international rock standards (DNC-1, BHVO-2 and BCR-2) indicate that precision and accuracy for trace elements are better than 10% of error.

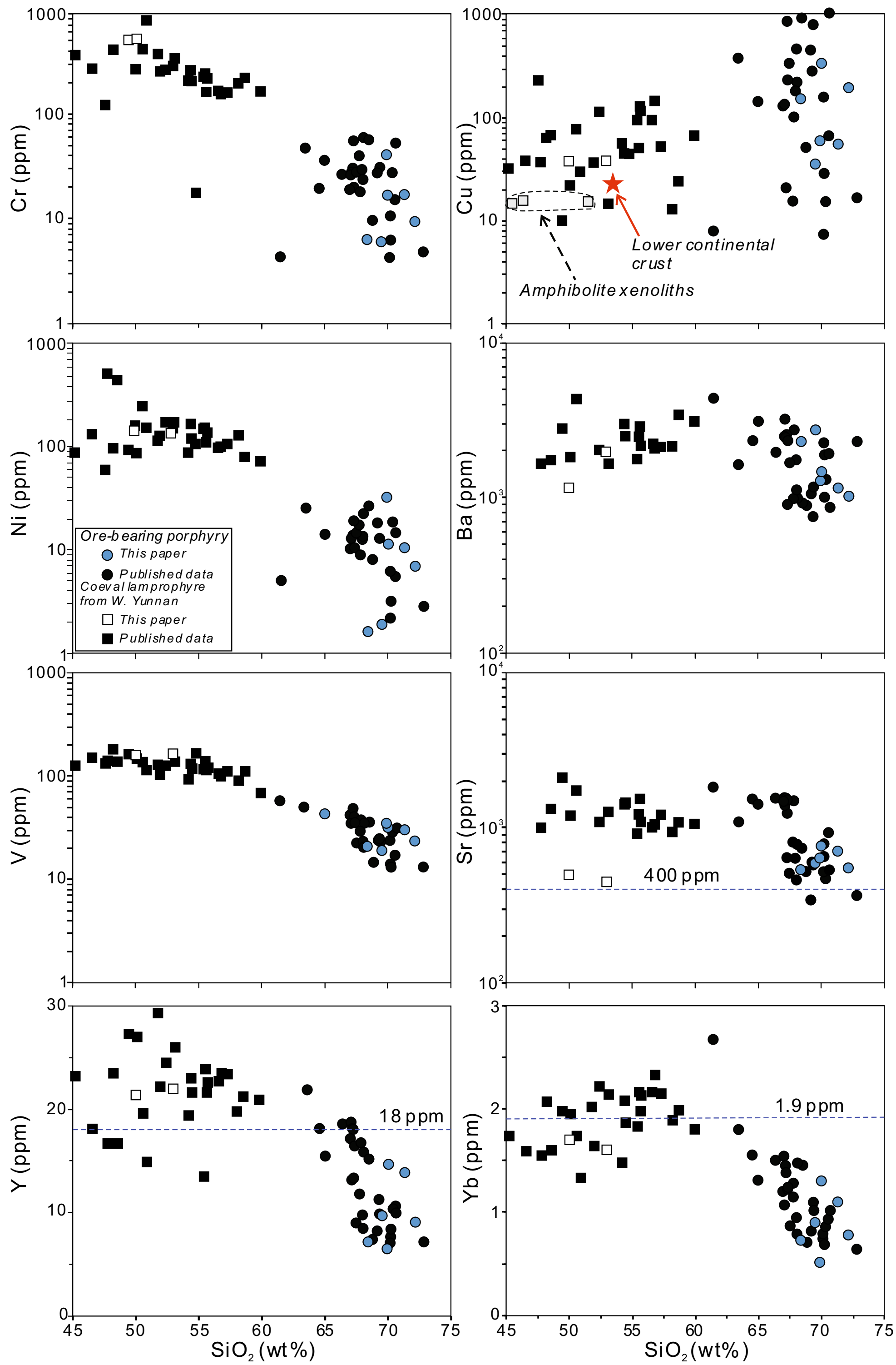

Fig. 5 SiO_2 vs. selected trace elements (ppm) for the studied lamprophyres and ore-bearing intrusions. Additional data sources are same as Fig. 3. Copper abundances of lower continental crust and the amphibolite xenoliths in the Liuhe porphyry are also shown for comparison. Their data sources: Rudnick and Gao (2003), Deng et al. (1998)

Whole-rock Sr-Nd isotope analysis

For Sr-Nd isotope analyses, chemical digestion and separation are performed in a Class 100 ultra-clean laboratory. 100 mg of the grounded sample powder was digested by a mixed solution of HNO_3 and HF in a Teflon beaker. Sr and Nd were separated from each other and purified through conventional cation-exchange chromatography. Sr-Nd isotopic ratio of each sample was measured in a Class 1000 ultra-clean laboratory. The Sr–Nd isotopic ratios of the purified solutions were determined on a Triton TI Thermal Ionization Mass Spectrometer (TIMS; Thermo Electron, Osterode, Germany) at the SKLGPMR, CUGW. The ratios of $^{87}Sr/^{86}Sr$ and $^{143}Nd/^{144}Nd$ ratios were normalized to $^{86}Sr/^{88}Sr = 0.1194$ and $^{146}Nd/^{144}Nd = 0.7219$, respectively. The $^{87}Sr/^{86}Sr$ ratios of the NBS987 Sr standards and $^{143}Nd/^{144}Nd$ ratios of the La Jolla Nd standards were determined as 0.710254 ± 0.000008 and 0.511856 ± 0.000012, respectively. The total analytical blanks for Sr and Nd isotopes are less than 100 pg and 60 pg, respectively.

Results

All porphyry samples in this study were found to have acid compositions and enriched in alkalis ($Na_2O + K_2O = 7.9$–11.2 wt.%) with higher K_2O/Na_2O ratios (mostly >1.0) (Fig. 3). These samples were plotted in the fields of shoshonite and high-K calc-alkaline rocks (Fig. 3b). All samples contain low total rare earth elements (REE) contents (67–269 ppm) and are relatively enriched in light rare earth elements (LREEs) with negligible Eu anomalies (Fig. 4a). Relative to high field strength elements (HFSEs), they are enriched in large ion lithophile elements (LILEs) with marked negative Ta-Nb-Ti anomalies (Fig. 4b). All samples are characterized by enrichment in Ba (mostly >1000 ppm), Sr (mostly >400 ppm) contents as well as depletion in Yb (< 1.9 ppm) and Y (mostly <18 ppm), with low contents of compatible elements (Fig. 5). The initial Sr ($^{87}Sr/^{86}Sr_i = 0.7067$ to 0.7075) and Nd ($\varepsilon_{Nd}(t) = -5.9$ to -1.7) isotopic ratios of these ore-bearing porphyries are similar to those of the coeval lamprophyres from *W. Yunnan* province (Fig. 6).

The two lamprophyric samples from the Beiya area have been altered to varying degrees after emplacement and show high loss on ignition (LOI) values (5.6–6.7). In this paper, published data of Paleogene lamprophyre samples from W. Yangtze are plotted for comparison. The *W. Yunnan* lamprophyres comprised low levels of TiO_2 and $Fe_2O_3^T$, variable compatible element contents, as well as high levels of K_2O and LILEs (e.g. Ba and Sr) relative to HFSEs, with steep REE patterns (Figs. 4, 5). These lamprophyres exhibit similar Sr-Nd isotopic compositions ($^{87}Sr/^{86}Sr_i = 0.7063$ to 0.7064; $\varepsilon_{Nd}(t) = -1.5$ to -1.4) to the ore-bearing porphyries (Fig. 6).

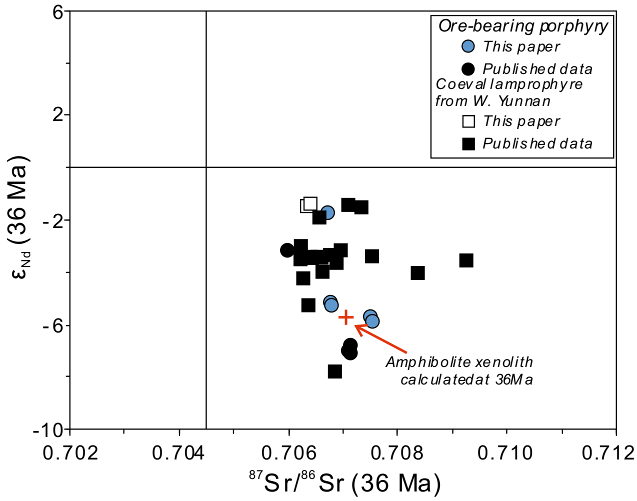

Fig. 6 $^{87}Sr/^{86}Sr$(36 Ma) vs. ε_{Nd}(36 Ma) diagram for the studied lamprophyres and ore-bearing intrusions. Published data sources are same as Fig. 3

Discussion

Ages of the ore-bearing porphyries

Laser ablation-inductively coupled plasma-mass spectrometry (LA-ICP-MS) U-Pb zircon dating of Beiya quartz syenite porphyry yielded an age of 36.5 ± 0.3 Ma, which was consistent with the Re-Os model age (36.9 ± 0.8 Ma) of molybdenite separated from the Beiya ore body (He et al. 2013). Lamprophyric dykes in Beiya were dated at 33.4 ± 0.6 Ma by the $^{39}Ar/^{40}Ar$ method (Xue et al. 2008). Similarly, a phlogopite collected from a lamprophyre at Yao'an produced an $^{40}Ar/^{39}Ar$ age of 33.4 ± 0.5 M (Lu et al. 2013b). $^{40}Ar/^{39}Ar$ dating of quartz and zircon LA-ICP-MS U-Pb dating of the Machangjing ore-bearing porphyries yielded emplacement ages between 40 Ma and 34 Ma (Peng et al. 2005; Liang et al. 2007; Lu et al. 2012). Based on the Re-Os dating method, molybdenites separated from the orebody show ages of 35.8 ± 1.6, 35.3 ± 0.7, and 33.9 ± 1.1 Ma, which were coeval with the ore-bearing porphyries (Wang et al. 2004a, b; Zeng et al. 2006; Guo et al. 2009; He et al. 2011). Lamprophyric dikes at Machangjing showed similar emplacement age of 36.2 ± 0.2 Ma (Lu et al. 2013b). Other ore-bearing porphyries in the western Yangtze, including Binchuan, Habo and Tongchang, are also determined to be coeval with the Beiya and Machangjing intrusions (Table 1).

All the potassic rocks in the western Yangtze have been considered to result from the magmatic response to lithospheric removal followed by asthenospheric upwelling (Lu et al. 2013a, b). The occurrence of the lamprophyres suggested local rather than complete removal of lithospheric mantle underneath the western Yangtze Block. High-resolution tomographic imaging of the crust and upper mantle under western Yangtze reveals a clear high-velocity anomaly at a depth between ~ 300 and 450 km from 100.5°E to 107°E (Liu et al. 2000; Fig. 7). The anomaly may refer to the delaminated lithospheric mantle. Thus, convective removal caused by Rayleigh-Taylor instability could most likely be a geodynamic process responsible for the formation of these rocks. It should be noted that all the potassic rocks were formed over a relatively short time span between 40 Ma and 32 Ma (Lu et al. 2013b; Liu et al. 2017). The tomographic image also reveals that the Yangtze Block has been subducted westward to 99°E and to a depth of 250 km (Fig. 7). Then we consider that the subducted lithosphere was blocking the continuous upwelling of the asthenosphere, which could be the reason for the short time span of the western Yangtze potassic rocks.

Origin of the ore-bearing porphyries

Coeval ore-bearing porphyries from the western Yangtze are discussed for comparison, which include the Binchuan, Habo and Tongchang intrusions (Table 1). All these porphyries exhibit similar Sr-Nd isotopic components and elemental signatures, such as the enrichment of K_2O, LREEs, LILEs, low compatible element contents, depletion of HREE and Y, as well as high K_2O/Na_2O and Sr/Y ratios (Figs. 2, 3, 4, 5 and 6), to intrusions that we studied. Thus, all the ore-bearing porphyries may share common petrogenesis. These ore-bearing porphyries show similar geochemical characteristics to adakite, distinguishing it from typical arc magma (Fig. 8), high Sr, Al_2O_3, Sr/Y and La/Yb ratios and low Yb and Y contents with the exception for K_2O.

Original partial melts of a metasomatic lithospheric mantle are generally low-SiO_2 adakite-like ($SiO_2 < 60$ wt.%, MgO > 4 wt.%) composition (Martin et al. 2005). All the ore-bearing porphyries show relatively high SiO_2 (mostly >65 wt.%) and low MgO (mostly <2 wt.%) contents (Table 2), arguing directly against the partial melting of lithospheric mantle (Table 3).

Partial melts derived from subducted slab are generally characterized by enrichment in sodium ($K_2O/Na_2O < 0.4$) and exhibit similar Sr-Nd isotopic ratios to MORB (Martin et al. 2005), which is in contrast to our samples (Figs. 3, 6). More importantly, the Yangtze Block had been located in an intra-continental position since the Triassic (Wang et al. 2000; Lu et al. 2015a). Thus, these adakite-like porphyries were unlikely to have originated from a subducted slab.

The typical elemental signatures (e.g., high K_2O, Ba and Sr contents), REE and trace element patterns of these felsic intrusions are also evidently present in the coeval lamprophyres (Figs. 3, 4, 5). And the similarity of Sr-Nd isotopic ratios between the ore-bearing intrusions and coeval lamprophyres indicates an AFC scenario (Fig. 6). In general, magmatic rocks derived by AFC process have a wide compositional range and exhibit inflections between elements on variation diagrams. However, in the western Yangtze, the Eocene to Oligocene magmatism is dominated by felsic components with the absence of intermediate rocks. In addition, the mafic rocks are relatively small volume in size and generally occur as dykes, making it unlikely for them to generate huge volumes of felsic magmas via AFC. If these porphyries were produced by the AFC of mafic magmas, the coherent decreasing trends in SiO_2 vs. Al_2O_3, Na_2O, CaO, Ba and Sr plots for the felsic rocks

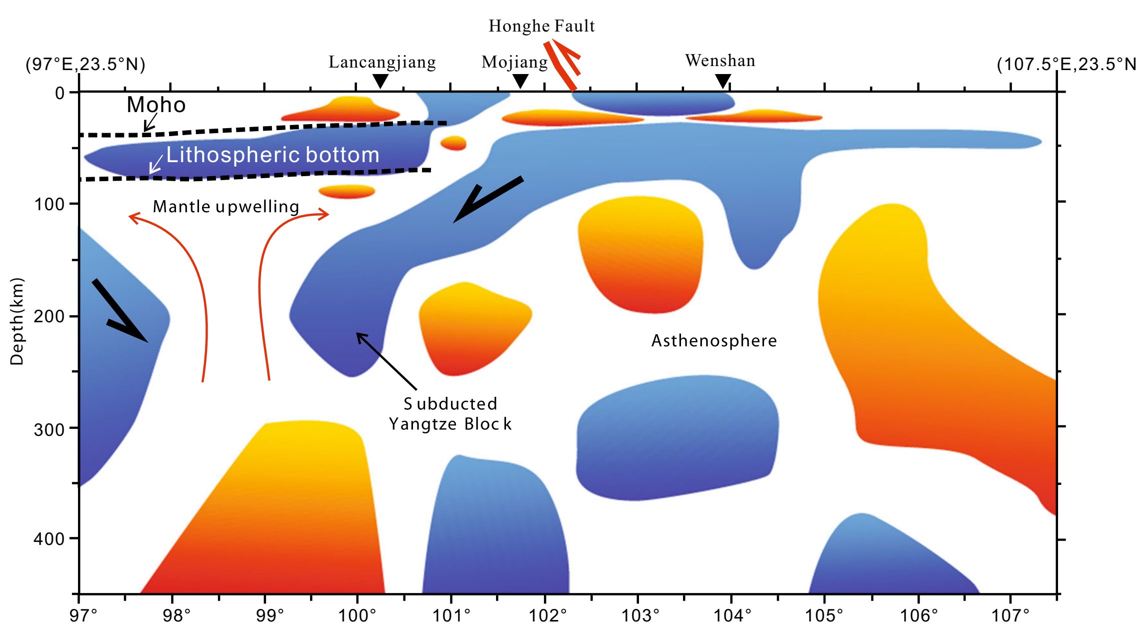

Fig. 7 A seismic tomographic section along latitude 23.5°N crossing western Yunnan (modified from Liu et al. (2000)). Blue areas represent high-velocity anomalies; Red areas represent low-velocity anomalies

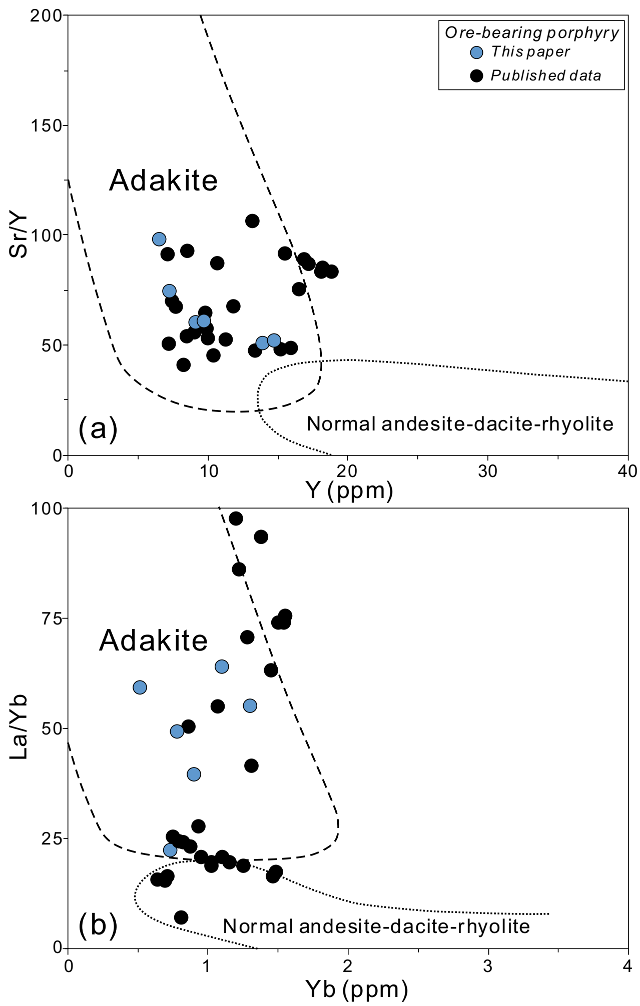

Fig. 8 Plots of (**a**) Sr/Y vs. Y (Defant and Drummond 1993), and (**b**) La/Yb vs. Yb (Castillo et al. 1999). Additional data sources are same as Fig. 3

would require significant removal of plagioclase (Figs. 5, 9), which was contradicted by the absence of negative Eu anomalies (Fig. 4). Thus, these ore-bearing porphyries are unlikely to have been generated by the AFC of mantle-derived basaltic magmas.

Kay and Kay (1993) proposed that partial melts of delaminated dense eclogitic lower crust interacted with mantle peridotite to produce adakite-like melts with high Sr/Y and La/Yb ratios during continent-continent collision. Due to the assimilation of mantle material, the resulting melts generally exhibit low SiO_2 (< 66 wt.%), elevated MgO (> 1.5 wt.%), Mg# (> 35) and compatible element contents (Fig. 10). But our samples have relatively high SiO_2 as well as low MgO, Cr and Ni contents than the rocks derived from delaminated lower crust. Furthermore, on the basis of seismic profiles, crustal thickness beneath western Yangtze Block is currently ca. 40–55 km (Li et al. 2008; Sun et al. 2008) (Fig. 11), approximately equivalent to that (ca. 45–55 km) in the Eocene (Zhao et al. 2003). This suggests that significant crustal delamination did not occur (Lu et al. 2013a). Thus, the petrogenesis of these ore-bearing rocks could not be satisfactorily explained by delaminated lower crustal melting.

These ore-bearing intrusions have similar Sr-Nd isotopic components as the lower crustal garnet-bearing amphibolite xenoliths, indicating that they were likely formed by partial melting of thickened mafic lower crust (Fig. 6). Miocene ore-bearing porphyries hosting post-collisional porphyry Cu deposits in the Himalayan orogenic belt have been attributed to the dehydration melting of garnet-bearing amphibolite in a thick lower crust (Hou et al. 2015, 2017). Ding et al. (2007) investigated two Eocene adakite-like intrusions (Xifanping and Zhiju) (ca. 35 Ma) from western Yangtze Block and argued that they were formed by partial melting of amphibolites (representing Neoproterozoic mafic rocks) in the thickened lower crust of the Yangtze block. Recently, Hou et al. (2017) investigated lower crustal amphibolite and garnet-bearing amphibolite xenoliths within the Beiya porphyry intrusion. They are interpreted as residuals of Neoproterozoic arc magmas pounding at the base of the Yangtze Block and are enriched in Cu and Au. Then, melting of the Neoproterozoic arc residuals at 40–30 Ma might supply metal endowment for the post-collisional porphyry system. Utilizing a geohygrometer for ore-bearing porphyries in the Himalaya orogenic belt, however, Lu et al. (2015b) demonstrated that these potassic high Sr/Y magmas had high dissolved H_2O contents >10 wt.%, which could not be explained simply by dehydration melting of amphibolites (maximum of 6.7 ± 1.4 wt.%) (Sen and Dunn 1994; Rapp and Watson 1995; Sisson et al. 2005). Furthermore, it should be noted that all the ore-bearing porphyries are potassic and have high K_2O content and K_2O/Na_2O ratio. However, experimental data on partial melting of amphibolites between 8 and 32 kbar found the resulting melts to be sodic with low K_2O contents (< 4 wt.%), and $K_2O/Na_2O < 1$ (Fig. 3; Sen and Dunn 1994; Rapp and Watson 1995; Moyen and Stevens 2005). Thus, these potassic ore-bearing porphyries are unlikely to have been derived from the garnet-bearing amphibolites. From here we see that an alternative source would be needed to account for the formation of these potassic, adakite-like ore-bearing porphyries.

All the samples have high K_2O content (mostly >4 wt.%) and K_2O/Na_2O ratio (mostly >1), while most are plotted in the fields of shoshonite (Fig. 4). Turner et al. (1996) have proposed that shoshonitic rocks are generally derived from subcontinental lithospheric mantle modified by introduction of slab-derived fluids. According to the experimental data of Wyllie and Sekine (1982), interaction between such fluids and mantle peridotite can produce hybrid pyroxenites consisting of pyroxene, garnet and potassic minerals (phlogopite and potassic amphibole). Subsequent partial melting of the hybridized mantle source can yield potassic mafic melts. However, as discussed above, the investigated porphyries were not directly produced by the AFC of mantle-derived

Table 2 Whole-rock main element oxide [wt.%], trace element and REE [ppm] contents of selected rock sample

	LOD	Machangjing							Beiya		Beiya lamprophyre	
		10MCQ01–1	10MCQ01–2	10MCQ01–4	10MCQ01–5	10MCQ01–11	10MCQ01–11*	Error (%)	11BY01–1	11BY02–1	11BY02–2	11BY02–3
Main element oxide												
SiO_2		69.90	72.15	68.45	70.00	71.32	70.9	0.58	69.52	68.38	52.96	50.00
TiO_2		0.32	0.24	0.32	0.30	0.30	0.31	3.33	0.26	0.25	0.67	0.66
Al_2O_3		15.37	14.33	15.38	14.93	14.94	15.50	3.74	16.39	17.66	15.94	15.69
Fe_2O_3		0.85	1.12	1.05	1.52	0.93	0.90	3.23	0.88	1.24	4.35	3.20
FeO		0.94	0.21	0.66	0.57	0.52	0.48	7.69	0.18	0.13	2.02	2.24
MnO		0.02	0.03	0.02	0.04	0.01	0.01	0.00	0.00	0.00	0.04	0.07
MgO		1.35	0.71	1.38	0.91	0.94	0.92	2.12	0.11	0.24	4.73	4.01
CaO		1.25	1.42	1.88	1.69	1.38	1.40	1.45	0.15	0.20	3.96	7.24
Na_2O		4.42	3.42	4.28	3.83	3.51	3.60	2.56	0.93	1.17	3.17	3.26
K_2O		4.15	5.02	4.05	5.19	5.04	5.25	4.17	10.24	6.72	4.61	4.62
P_2O_5		0.11	0.09	0.11	0.13	0.14	0.14	0.00	0.07	0.03	0.84	0.82
LOI		1.06	1.13	2.28	0.65	0.79	0.75	5.06	1.72	4.21	5.62	6.69
Total		99.74	99.87	99.86	99.76	99.82	100.15	0.33	100.45	100.23	99.57	99.14
Trace elements and REEs												
Cu	0.0015	59.44	196.28		340.13	55.58	52.23	6.23	35.84	154.16	38.71	38.13
Ba	0.0002	1288.08	1024.92		1476.08	1158.27	1179.30	1.82	2738.49	2306.33	1968.70	1164.28
Rb	0.0000	270.79	248.06		228.26	203.58	199.40	2.05	408.94	255.80	178.27	181.53
Sr	0.0000	640.10	550.18		764.21	706.55	720.20	1.93	591.38	538.34	448.42	494.94
Y	0.0001	6.52	9.11		14.70	13.89	14.10	1.51	9.72	7.22	21.99	21.38
Zr	0.0236	149.22	94.29		114.09	132.94	125.43	5.65	176.86	173.24	91.30	89.26
Nb	0.0016	4.88	10.62		14.41	14.00	14.23	1.64	11.73	12.68	6.62	6.48
Th	0.0000	17.17	22.01		32.87	33.15	34.64	4.49	14.82	14.92	9.65	9.38
Pb	0.0000	11.66	17.39		26.42	20.71	19.50	5.84	659.17	157.68	27.12	25.57
Ga	0.0001	20.85	19.09		19.12	19.16	18.70	2.40	19.89	21.56	19.54	19.21
Ni	0.0015	32.17	6.88		11.27	10.49	10.73	2.29	1.88	1.61	149.04	158.78
V	0.0005	34.95	23.43		31.57	30.13	29.80	4.41	19.06	20.71	164.23	159.02
Cr	0.0026	40.71	9.40		16.90	17.12	18.49	8.00	6.03	6.35	285.48	266.86
Hf	0.0002	4.13	3.27		3.66	4.07	4.11	0.98	4.93	5.04	2.44	2.38
Ta	0.0000	0.39	0.97		1.14	1.15	1.21	5.21	0.68	0.78	0.42	0.41

Table 2 (continued)

	LOD	Machangjing							Beiya		Beiya lamprophyre	
		10MCQ01–1	10MCQ01–2	10MCQ01–4	10MCQ01–5	10MCQ01–11	10MCQ01–11*	Error (%)	11BY01–1	11BY02–1	11BY02–2	11BY02–3
U	0.0000	4.53	5.65		9.86	7.55	7.34	2.78	4.40	3.45	3.45	4.87
La	0.0001	30.45	38.40		71.81	70.29	72.97	3.81	35.66	16.30	29.38	28.04
Ce	0.0001	54.44	67.21		123.73	120.52	115.63	4.06	58.40	28.72	62.57	58.58
Pr	0.0002	6.19	7.21		12.45	11.96	12.13	1.42	6.48	3.16	7.07	6.75
Nd	0.0005	21.70	24.65		41.76	39.08	36.12	7.57	21.42	11.04	28.56	27.36
Sm	0.0021	3.48	4.02		6.38	6.01	6.54	8.81	3.55	2.06	5.69	5.27
Eu	0.0004	1.00	1.00		1.54	1.31	1.29	1.53	1.19	0.80	1.85	1.67
Gd	0.0002	2.47	2.92		4.46	4.18	4.09	2.15	2.59	1.68	4.92	4.87
Tb	0.0001	0.29	0.35		0.57	0.52	0.55	5.77	0.36	0.25	0.74	0.74
Dy	0.0009	1.32	1.74		2.74	2.53	2.56	1.19	1.82	1.34	3.93	3.95
Ho	0.0003	0.22	0.31		0.50	0.46	0.48	4.35	0.34	0.25	0.72	0.73
Er	0.0015	0.61	0.84		1.30	1.20	1.21	0.83	0.93	0.69	1.86	1.89
Tm	0.0002	0.08	0.12		0.19	0.17	0.17	0.00	0.14	0.10	0.26	0.26
Yb	0.0012	0.51	0.78		1.30	1.10	1.12	1.81	0.90	0.73	1.60	1.70
Lu	0.0004	0.08	0.12		0.19	0.19	0.20	5.26	0.13	0.11	0.24	0.24

LOD limit of detection; *duplicate; ‘Error’ represents relative error between analyzed and duplicate values. Unit is ppm for LOD

Table 3 Sr-Nd isotopic components of selected rock samples

Intrusion	Machangjing			Beiya		Beiya lamprophyre	
Sample	10MCQ01–1	10MCQ01–2	10MCQ01–11	11BY01–1	11BY02–1	11BY02–2	11BY02–3
$^{87}Rb/^{86}Sr$	1.2239	1.3044	0.8336	2.0006	1.3746	1.1500	1.0609
$^{87}Sr/^{86}Sr$	0.707361	0.707473	0.707203	0.708520	0.708235	0.706991	0.706884
±2σ	7	12	13	10	8	8	10
$^{147}Sm/^{144}Nd$	0.0969	0.0985	0.0930	0.1009	0.1134	0.1213	0.1173
$^{143}Nd/^{144}Nd$	0.512525	0.512345	0.512349	0.512323	0.512317	0.512549	0.512544
±2σ	5	8	5	5	7	7	6
$(^{87}Sr/^{86}Sr)_i$	0.7067	0.7068	0.7068	0.7075	0.7075	0.7064	0.7063
$\varepsilon_{Nd}(T)$	−1.7	−5.3	−5.1	−5.7	−5.9	−1.4	−1.5

magmas or partial melting of a modified lithospheric mantle. They were most likely generated by partial melting of underplated potassic mafic rocks that originated from a modified lithospheric mantle which will be discussed below.

The investigated porphyries have similar Sr-Nd isotopic characteristics to the coeval lamprophyres which have been interpreted as products of partial melting of the enriched subcontinental lithospheric mantle modified by previous subduction (Li et al. 2002; Lu et al. 2015a). It should be noted that these lamprophyres are also shoshonitic, have high K_2O/Na_2O ratios >1 (Fig. 3) and contain potassic minerals (amphibole and phlogopite). It was possible that part of the Eocene potassic melts intruded the crust to yield lamprophyric dykes with the rest underplating beneath continental lower crust to form juvenile crust. Subsequently, partial melting of the potassic juvenile crust might have produced the potassic ore-bearing porphyries. Experimental data also indicated that the partial melting of high-potassium basaltic rocks could produce some adakite-like melts with relatively high K_2O/Na_2O ratios (Rapp and Watson 1995; Sisson et al. 2005). The enrichment in Sr and the absence of significant Eu anomalies in our samples necessitate a source beyond the plagioclase stability field (Fig. 4 and Fig. 5). Furthermore, these ore-bearing porphyries exhibit relatively low HREE (Yb = 0.51 to 1.98 ppm), Y (6.5 to 18.8 ppm) contents (Fig. 5) and relatively steep HREE patterns (Gd_N/Yb_N = 1.1–2.2), indicating that garnet rather than amphibole is residual in the source (Halla et al. 2009). The low-HREE TTGs of Halla et al. (2009) share similar signatures of HREEs to the ore-bearing porphyries. The former has been interpreted as products of high-P (>2.0 Gpa) partial melting of a garnet-bearing basaltic source. However, they exhibit lower Yb (average 0.4 ppm), Y (average 4.5 ppm) and higher Gd_N/Yb_N (average 4.0), indicating that the ore-bearing porphyries have a shallower source than the low-HREE TTGs. Garnet can be produced via the breakdown of amphibole + plagioclase under fluid-free conditions at pressures between 12 kbar and 18 kbar (Rushmer 1993), while amphibole remains stable with garnet up to at least 15 kbar (ca. 50 km) (Patiño Douce and Beard 1995). The presence of garnet rather than amphibole and plagioclase as the dominant residual mineral phase therefore requires a thickened lower crustal source

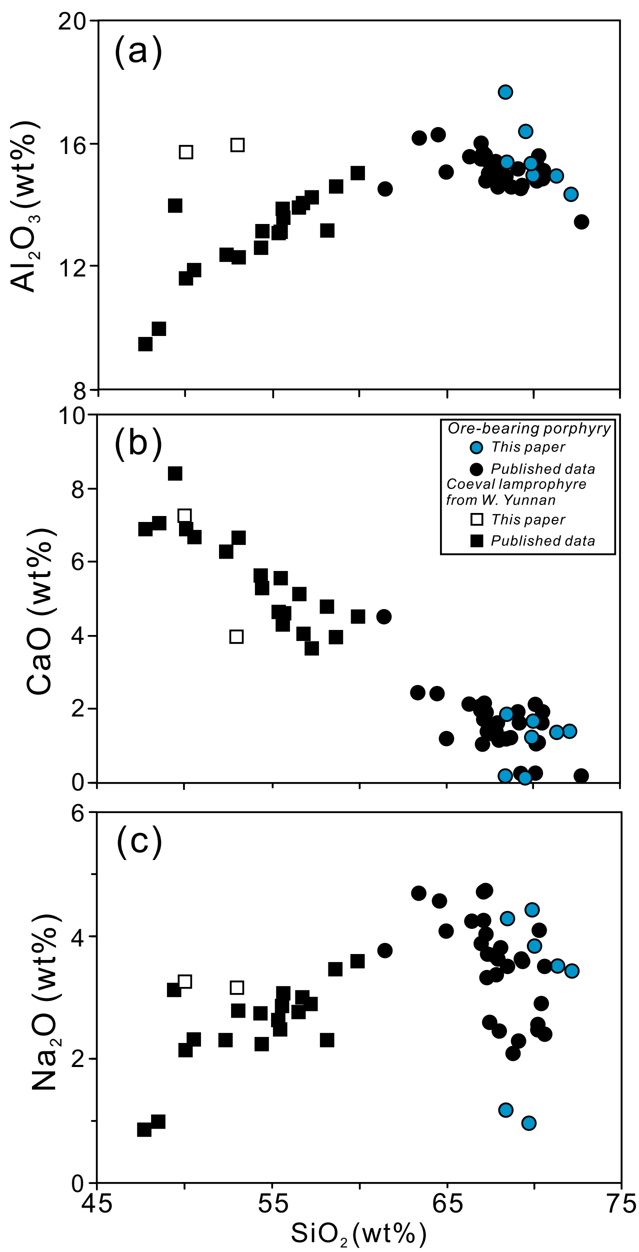

Fig. 9 Plot of Al_2O_3 (**a**), CaO (**b**) and Na_2O (**c**) vs. SiO_2 diagrams for the studied lamprophyres and felsic intrusions. Additional data sources are same as Fig. 3

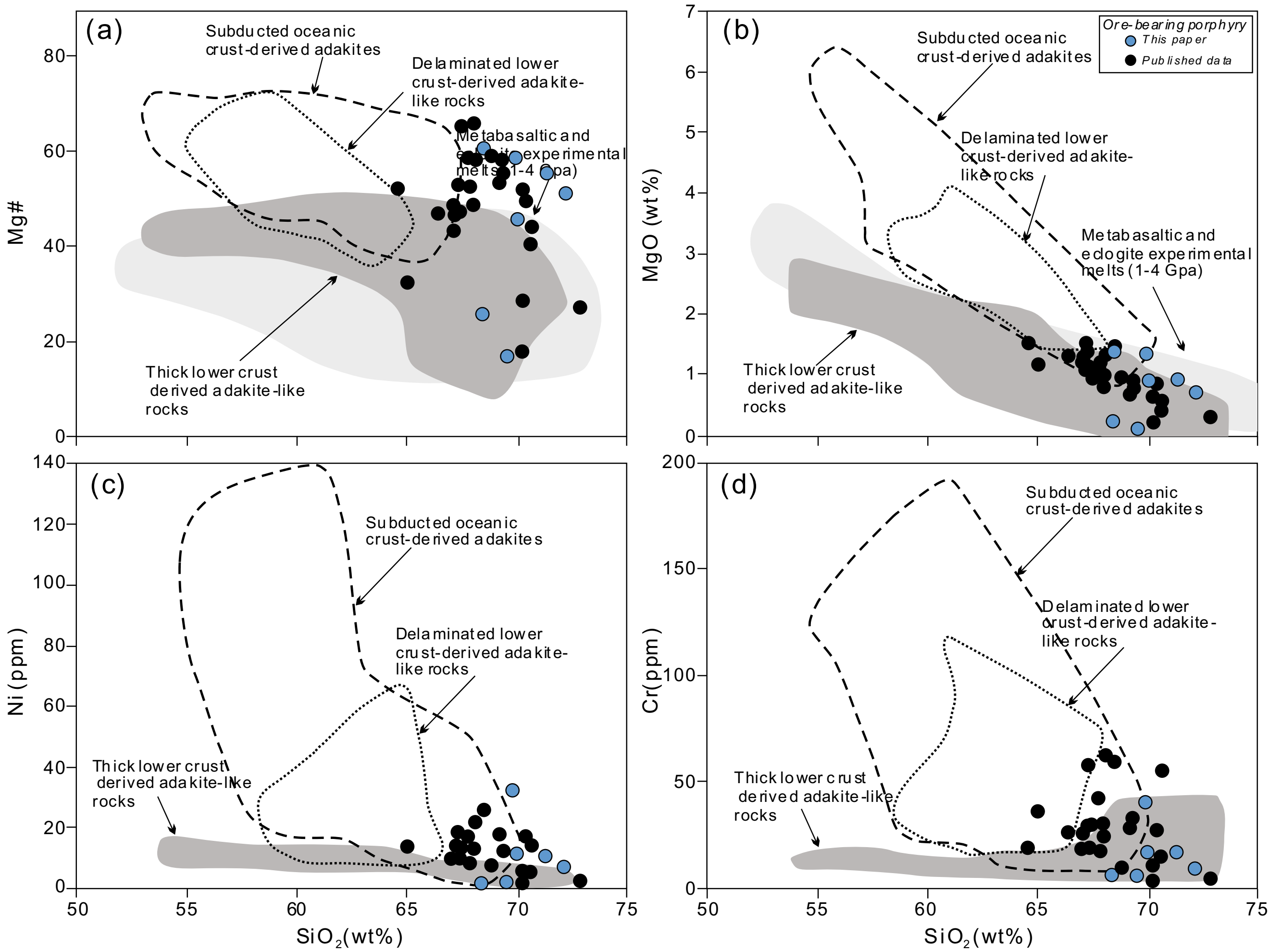

Fig. 10 **a** Mg#, (**b**) MgO (wt.%), (**c**) Ni (ppm) and (**d**) Cr (ppm) vs. SiO_2 (wt.%) (modified from Wang et al. (2006)). Additional data sources are same as Fig. 3

(its depth ≥ 50 km), most probably under eclogite-facies conditions. The occurrence of eclogite xenoliths within the Eocene Liuhe porphyry intrusion also implied that western Yangtze Block had a thickened lower crust during the Eocene (Cai 1992). Estimated pressure of the garnet-bearing xenoliths within the Eocene Liuhe porphyry also supported the speculation that western Yangtze Block had a thick crust (~ 45–55 km in depth) (Zhao et al. 2004). Compared to those adakite-like rocks derived from thick lower crust and experimental melts of metabasaltic rocks and eclogites, the less felsic ore-bearing porphyries have slightly higher Mg#, Cr and Ni contents (Fig. 10), indicating a mixing of mantle-derived magmas. This speculation is also corroborated by the negative correlation between $^{87}Sr/^{86}Sr_i$ and $\varepsilon_{Nd}(t)$ (Fig. 6), and the occurrence of mantle-derived mafic enclaves in the Machangjing intrusion (Guo et al. 2012). But the mixing was likely limited because (1) the ore-bearing porphyries have relatively low MgO contents (Fig. 10b); and (2) the coeval lamprophyres and ore-bearing porphyries exhibit divergent trends in the plots of SiO_2 vs. Al_2O_3 and Na_2O (Fig. 9). Thus, the investigated ore-bearing porphyries were likely to have been produced by partial melting of the underplated potassic mafic rocks, with limited mixing of mantle-derived magmas.

Implications for the genesis of the porphyry copper deposits in non-subducting setting

Slab melts are unusually oxidized, enriched in sulfur (Oyarzun et al. 2001) and water (Sajona and Maury 1998), and contain high initial Cu contents (Sun et al. 2011, 2012a, b). These characteristics provide a plausible explanation why most porphyry Cu deposits are hosted by adakites and occur in subduction settings. In this contribution, however, the ore-bearing adakite-like porphyries might have been derived by the partial melting of newly underplated potassic mafic rocks under post-collisional setting, instead of slab melting at subducting zone. As mentioned above, these latent underplated rocks and lamprophyric dykes in western Yangtze shared the same metasomatic lithospheric mantle source, which had been modified

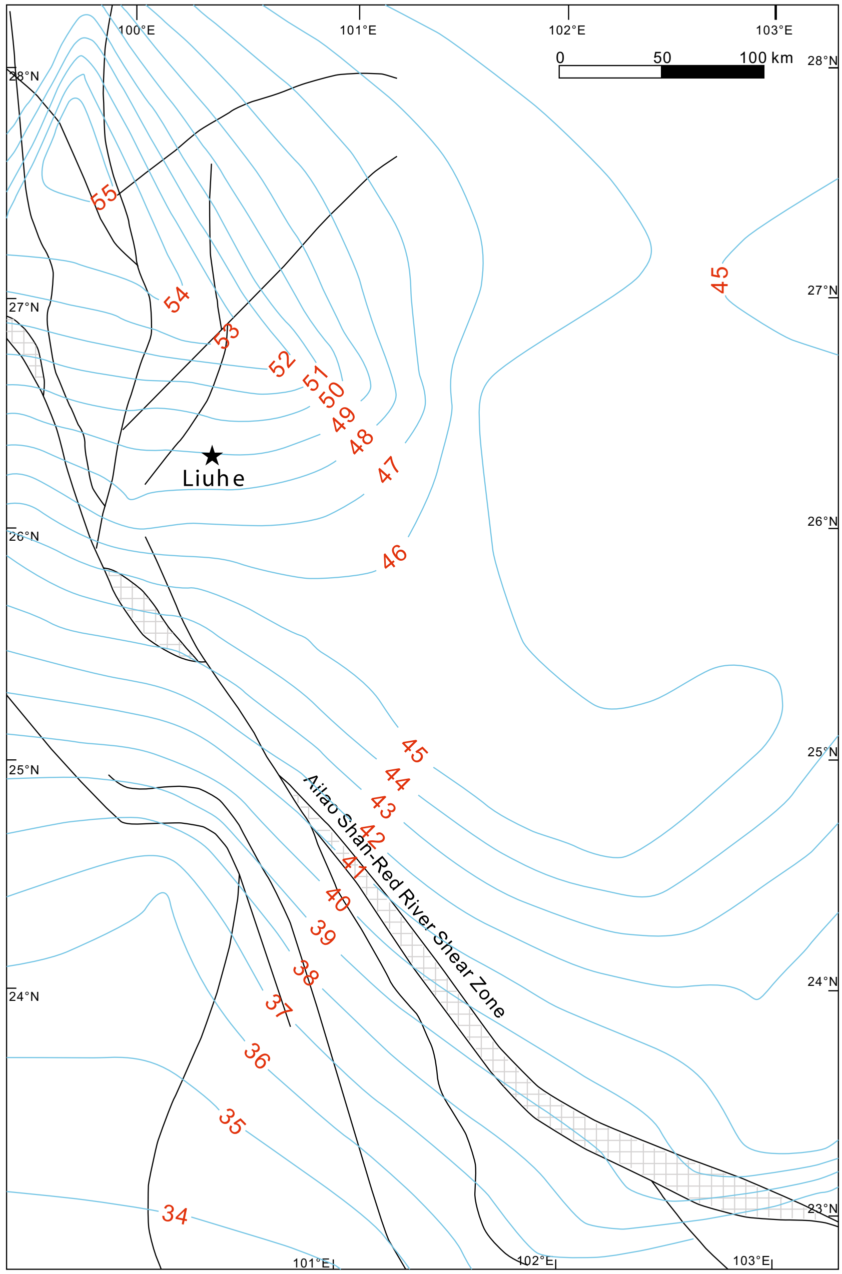

Fig. 11 The Moho depth (km) across western Yangtze and its adjacent region (Li et al. 2008). Location of the xenoliths in the Liuhe porphyry is also exhibited in the Figure

by materials released from subducted slabs. The lithospheric mantle underneath the *W. Yunnan* has undergone a series of subduction-related metasomatic events: (1) the Neoproterozoic slab subduction related to the formation of the Panxi–Hannan arc (Zhao et al. 2011; Zhou et al. 2002, 2006); (2) the subduction of the Paleo-Tethyan oceanic slab during the Paleozoic (Guo et al. 2005); (3) the Neo-Tethyan subduction (Lei et al. 2009). These slab-derived fluids would infiltrate into the overlying mantle wedge and undergo hybridization with peridotite to form metasomatic mantle domains (Fig. 12a), composed of a series of discrete veins or masses (Wyllie and Sekine 1982). Such processes would enable the hybridized mantle domains to inherit the elevated oxygen fugacity as well as high contents of water, sulfur and copper copper from the slab fluids. Subsequently, partial melting of these mantle domains would be responsible for the formation of the newly underplated potassic rocks (Fig. 12b). The presence of phlogopite, amphibole and magnetite in the lamprophyres suggests that the underplated rocks have high oxygen fugacity and water content. Compared to lower continental crust (26 ppm; Rudnick and Gao 2003) and the amphibolite xenoliths in the Liuhe porphyry (~ 14–15 ppm; Deng et al. 1998), most of these lamprophyres show a higher Cu abundance (62.7 ppm in average) (Fig. 5). Thus, we concluded that the newly underplated potassic rocks have high metallogenic potential.

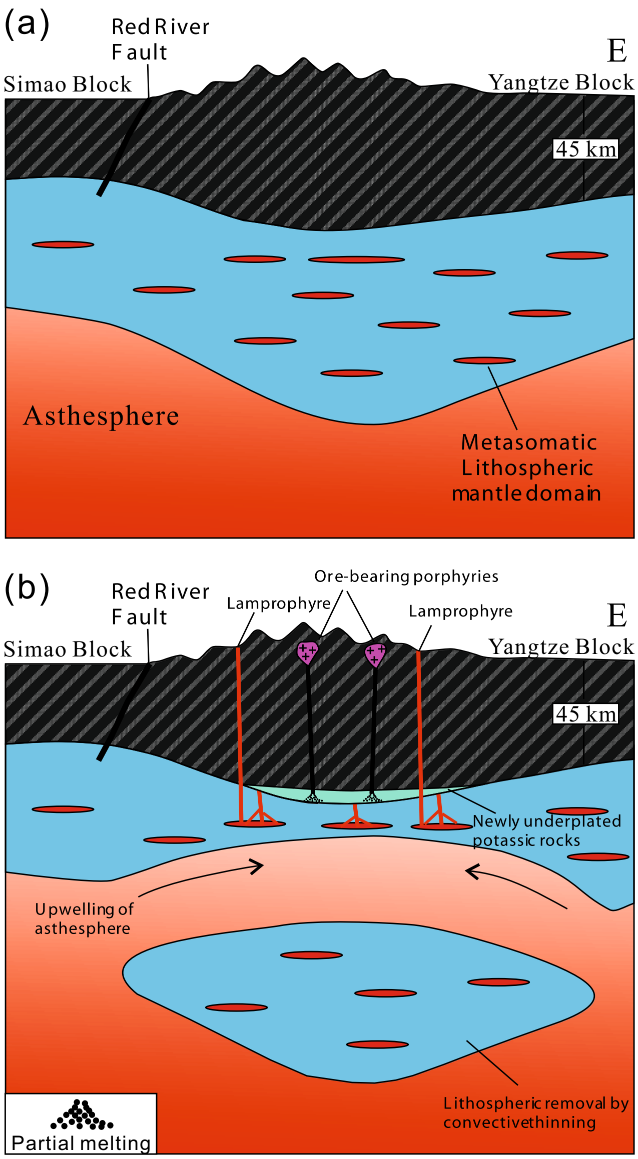

Fig. 12 Geodynamic model for the formation of these ore-bearing porphyries. **a** Thicken lithosphere underneath the western Yangtze Block after the Indo-Asian collision. **b** Convective removal for lithospheric root of the western Yangtze Block at ~ 40–32 Ma

Conclusions

(1) The investigated Eocene potassic ore-bearing porphyries exhibit adakitic affinities such as depletion in HREE, absence of negative Eu anomaly, high Sr/Y, La/Yb and low Y, Yb abundances.
(2) They were probably derived by partial melting of newly underplated potassic mafic rocks.
(3) We propose that all the studied potassic rocks were emplaced in a post-collisional setting, associated with the local removal of lithospheric mantle.

Acknowledgments We are grateful to M.A.T.M. Broekmans (Editor in Chief), X.S. Xu (Associate Editor), Lhiric Agoyaoy (JEO Assistant), Esa Heilimo and other anonymous reviewers for their thoughtful reviews and constructive comments. This study was financially supported by the National Natural Science Foundation of China (No. 41703022).

References

Boynton WV (1984) Cosmochemistry of the rare earth elements: meteorite studies. In: Henderson, P. (eds), Rare Earth Element Geochemistry. Elsevier, Amsterdam, pp 63–114.

Cai XP (1992) Discovery of deep-derived xenoliths in Cenozoic alkali-rich porphyries along the margin of the Yangtze Platform and its significance. Sci Geol Sin 2:183–189 (in Chinese with English abstract)

Castillo PR, Janney PE, Solidum RU (1999) Petrology and geochemistry of Camiguin island, southern Philippines: insights to the source of adakites and other lavas in a complex arc setting. Contrib Mineral Petrol 134:33–51

Defant MJ, Drummond MS (1990) Derivation of some modern arc magmas by melting of young subducted lithosphere. Nature 347: 662–665

Defant MJ, Drummond MS (1993) Mount St. Helens: potential example of the partial melting of the subducted lithosphere in a volcanic arc. Geology 21:547–550

Defant MJ, Kepezhinskas P (2001) Adakites: a review of slab melting over the past decade and the case for a slab-melt component in arcs. EOS, Trans 82:65–69

Deng WM, Huang X, Zhong DL (1998) Petrological characteristics and genesis of Cenozoic alkali-rich porphyry in West Yunnan, China. Sci Geol Sin 33:412–425 (in Chinese with English abstract)

Deng J, Wang QF, Li GJ, Santosh M (2014) Cenozoic tectono-magmatic and metallogenic processes in the Sanjiang region, southwestern China. Earth Sci Rev 138:268–299

Ding L, Kapp P, Yue Y, Lai Q (2007) Postcollisional calc-alkaline lavas and xenoliths from the southern Qiangtang terrane, central Tibet. Earth Planet Sci Lett 254:28–38

Gao S, Ling WL, Qiu YM, Lian Z, Hartmann G, Simon K (1999) Constrasting geochemical and Sm-Nd isotopic compositions of Archean metasediments from the Kongling high-grade terrain of the Yangtze craton: evidence for cratonic evolution and redistribution of REE during crust anatexis. Geochim Cosmochim Acta 63: 2071–2088

Guo ZF, Hertogen J, Liu JQ, Pasteels P, Boven A, Punzalan L, He HY, Luo XJ, Zhang WH (2005) Potassic magmatism in western Sichuan and Yunnan provinces, SE Tibet, China: petrological and geochemical constraints on petrogenesis. J Petrol 46:33–78

Guo F, Fan W, Li C (2006) Geochemistry of late Mesozoic adakites from the Sulu belt, eastern China: magma genesis and implications for crustal recycling beneath continental collisional orogens. Geol Mag 143:1–13

Guo XD, Wang ZH, Chen X, Wang X, Wang SX (2009) Machangqing porphyry-type Cu-Mo-Au deposit, Yunnan province: geological characteristics and genesis. Acta Geol Sin 83:1901–1914 (in Chinese with English abstract)

Guo XD, Ge LS, Wang L, Wang ZH, Shi XC (2012) Characteristics of deep-derived enclave and its zircon LA-ICP-MS U-Pb age of Machangqing complex, Yunnan Province. Acta Petrol Sin 28: 1413–1424

Halla J, Hunen JV, Heilimo E, Hölttä (2009) Geochemical and numeriacal constraints on Neoarchean plate tectonics. Precambrian Res 174: 155–162

He WY, Mo XX, Yu XH, Li Y, Huang XK, He ZH (2011) Geochronological study of magmatic intrusions and mineralization of Machangqing porphyry Cu-Mo-Au deposit, western Yunnan province. Earth Science Frontiers 18:207–215

He WY, Yu XH, Mo XX, He ZH, Li Y, Huang XK, Su GS (2012) Genetic types and the relationship between alkali-rich intrusion and mineralization of Beiya gold-polymetallic ore field, western Yunan Province, China. Acta Petrol Sin 28:1401–1412 (in Chinese with English abstract)

He WY, Mo XX, Yu XH, He ZH, Dong GC, Liu XB, Su GS, Huang XF (2013) Zircon U-Pb and molybdenite Re-Os dating for the Beiya gold-polymetallic deposit in the western Yunnan Province and its geological significance. Acta Petrol Sin 29:1301–1310

Hou ZQ, Ma HW, Khin Z, Zhang YQ, Wang MJ (2003) The Himalayan Yulong porphyry copper belt: produced by large-scale strike-slip faulting at eastern Tibet. Econ Geol 98:125–145

Hou ZQ, Gao YF, Qu XM, Rui ZY, Mo XX (2004) Origin of adakitic intrusives generated during mid-Miocene east-west extension in southern Tibet. Earth Planet Sci Lett 220:139–155

Hou ZQ, Yang ZM, Qu XM, Meng XJ, Li ZQ, Beaudoin G, Rui ZY, Gao YF, Zaw K (2009) The Miocene Gangdese porphyry copper belt generated during post-collisional extension in the Tibetan orogen. Ore Geol Rev 36:25–51

Hou ZQ, Yang ZM, Lu YJ, Kemp A, Zheng YC, Li QY, Tang JX, Yang ZS, Duan LF (2015) Subduction- and conllision-related porphyry Cu deposits in Tibet: possible genetic linkage. Geology 43:247–250

Hou ZQ, Zhou Y, Wang R, Zheng YC, He WY, Zhao M, Evans NJ, Weinberg RF (2017) Recycling of metal-fertilized lower continental crust: origin of non-arc Au-rich porphyry deposits at cratonic edges. Geology 45:563–566

Jiang YH, Jiang SY, Ling HF, Dai BZ (2006) Low-degree melting of a metasomatized lithospheric mantle for the origin of Cenozoic Yulong monzogranite-porphyry, east Tibet: geochemical and Sr-Nd-Pb-Hf isotopic constraints. Earth Planet Sci Lett 241:617–633

Jiang YH, Liu Z, Jia RY, Liao SY, Zhou Q, Zhao P (2012) Miocene potassic granite-syenite association in western Tibetan plateau: implications for shoshonitic and high Ba-Sr granite genesis. Lithos 134-135:146–162

Kay RW, Kay SM (1993) Delamination and delamination magmatism. Tectonophysics 219:177–189

Le Maitre RW (2002) Igneous rocks: a classification and glossary of terms, 2nd edn. Cambridge Univ. Press, Cambridge, p 236

Lei JS, Zhao DP, Su YJ (2009) Insight into the origin of the Tengchong intraplate volcano and seismotectonics in southwest China from local and teleseismic data. J Geophys Res 114:B05302

Li XH, Zhou HW, Chung SL, Lo CH, Wei GJ, Liu Y, Lee CY (2002) Geochemical and Sr-Nd isotopic characteristics of late Paleogene ultrapotassic magmatism in southeastern Tibet. Int Geol Rev 44: 559–574

Li YH, Wu QJ, Zhang RQ, Tian XB, Zeng RS (2008) The crust and upper mantle structure beneath Yunnan from joint inversion of receiver functions and Rayleigh wave dispersion data. Phys Earth Planet Inter 170:134–146

Li XH, Li ZX, Li WX, Wang XC, Gao YY (2013) Revisiting the "C-type adakites" of the Lower Yangtze River Belt, central eastern China: in-situ zircon Hf-O isotope and geochemical constraints. Chem Geol 345:1–15

Liang HY, Campbell IH, Allen CM, Sun WD, Yu HX, Xie YW, Zhang YQ (2007) The age of the potassic alkaline igneous rocks along the Ailao Shan-Red River shear zone: implications of the onset age of left-lateral shearing. J Geol 115:231–242

Liu FT, Liu JH, Zhong DL, He JK, You QY (2000) The subducted slab of Yangtze continental block beneath the Tethyan orogen in western Yunnan. Chin Sci Bull 45:466–472

Liu Z, Liao SY, Wang JR, Ma Z, Liu YX, Wang DB, Tang Y, Yang J (2017) Petrogenesis of late Eocene high Ba-Sr potassic rocks from western Yangtze block, SE Tibet: a magmatic response to the Indo-Asian collision. J Asian Earth Sci 135:95–109

Lu YJ, Kerrich R, Cawood PA, McCuaig TC, Hart CJR, Li ZX, Hou ZQ, Bagas L (2012) Zircon SHRIMP U-Pb geochronology of potassic felsic intrusions in western Yunnan, SW China: constraints on the relationship of magmatism to the Jinsha suture. Gondwana Res 22: 737–747

Lu YJ, Kerrich R, McCuaig TC, Li ZX, Hart CJR, Cawood PA, Hou ZQ, Bagas L, Cliff J, Belousova EA, Tang SH (2013a) Geochemical, Sr-Nd-Pb, and zircon Hf-O isotopic compositions of Eocene-Oligocene shoshonitic and potassic adakite-like felsic intrusions in western Yunnan, SW China: petrogenesis and tectonic implications. J Petrol 54:1309–1348

Lu YJ, Kerrich R, Kemp AIS, Mccuaig TC, Hou ZQ, Hart CJ, Li ZX, Cawood PA, Bagasi L, Yang ZM, Cliff J, Belousov EA, Jourdan F, Evans NJ (2013b) Intracontinental Eocene-Oligocene porphyry Cu mineral systems of Yunnan, western Yangtze Craton, China: compositional characteristics, sources, and implications for continental collision metallogeny. Econ Geol 108:1541–1576

Lu YJ, McCuaig TC, Li ZX, Jourdan F, Hart CJR, Hou ZQ, Tang SH (2015a) Paleogene post-collisional lamprophyres in western Yunnan, western Yangtze Craton: mantle source and tectonic implications. Lithos 233:139–161

Lu YJ, Loucks RR, Fiorentini ML, Yang ZM, Hou ZQ (2015b) Fluid flux melting generated postcollisional high Sr/Y copper ore-forming water-rich magmas in Tibet. Geology 43:583–586

Martin H, Smithies RH, Rapp R, Moyen JF, Champion D (2005) An overview of adakite, tonalite–trondhjemite–granodiorite (TTG), and sanukitoid: relationships and some implications for crustal evolution. Lithos 79:1–24

McDonough WF, Sun SS (1985) Isotopic and geochemical systematics in tertiary-recent basalts from southeastern Australia and implication for the subcontinental lithosphere. Geochim Cosmochim Acta 49: 2051–2067

Metcalfe I (2013) Gondwana dispersion and Asian accretion: tectonic and palaeogeographic evolution of eastern Tethys. J Asian Earth Sci 66: 1–33

Moyen JF (2009) High Sr/Y and La/Yb ratios: the meaning of the "adakitic signature". Lithos 112:556–574

Moyen JF (2011) The composite Archaean grey gneisses: petrological significance, and evidence for a non-unique tectonic setting for Archaean crustal growth. Lithos 123:21–36

Moyen JF, Stevens G (2005) Experimental constraints on TTG petrogenesis: Implications for Archaean geodynamics. In: Benn K, Mareschal JC, Condie K (eds) Archaean Geodynamics and Environment, vol. 164. AGU, Washington, pp 149–175

Oyarzun R, Márquez A, Lillo J, López I, Rivera S (2001) Giant versus small porphyry copper deposits of Cenozoic age in northern Chile: Adakitic versus normal calc-alkaline magmatism. Mineral Deposita 36:794–798

Patiño Douce AE, Beard JS (1995) Dehydration-melting of biotite gneiss and quartz amphibolite from3 to 15 kbar. J Petrol 36:707–738

Peccerillo A, Taylor SR (1976) Geochemistry of Eocene calc-alkaline volcanic rocks from the Kastamonu area, northern Turkey. Contrib Mineral Petrol 58:63–81

Peng JT, Bi XW, Hu RZ, Wu KX, Sang HQ (2005) Determination of ore- and rock-forming time of the Machangqing porphyry Cu (Mo) deposit, western Yunnan province. Acta Mineral Sin 25:69–74 (in Chinese with abstract)

Rapp RP, Watson EB (1995) Dehydration melting of metabasalt at 8~32 kbar: implications for continental growth and crust-mantle recycling. J Petrol 36:891~931

Rapp RP, Xiao L, Shimizu N (2002) Experimental constraints on the origin of potassium-rich adakites in eastern China. Acta Petrol Sin 18:293–302

Richards JP (2011a) High Sr/Y arc magmas and porphyry Cu±Mo±Au deposits: just add water. Econ Geol 106:1075–1081.

Richards JP (2011b) Magmatic to hydrothermal metal fluxes in convergent and collided margins. Ore Geol Rev 40:1–26
Richards JP, Kerrich R (2007) Adakite-like rocks: their diverse origins and questionable role in metallogenesis. Econ Geol 102:534–576
Rudnick RL, Gao S (2003) Composition of the continental crust. In: Heinrich DH, Turekian KK (eds) Treatise on geochemistry. Pergamon, Oxford, pp 1–64
Rushmer T (1993) Experimental high-pressure granulites: some applications to natural mafic xenolith suites and Archean granulite terranes. Geology 21:411–414
Sajona FG, Maury RC (1998) Association of adakites with gold and copper mineralization in the Philippines. Comptes rendus de l'Académie des sciences. Série II, Sciences de la terre et des planètes 326:27–34
Sen C, Dunn T (1994) Dehydration melting of a basaltic composition amphibolite at 1.5 and 2.0 GPa: implications for the origin of adakites. Contrib Mineral Petrol 117:394–409
Sillitoe RH (2010) Porphyry copper system. Econ Geol 105:3–41
Sisson TW, Ratajeski K, Hankins WB, Glazner AF (2005) Voluminous granitic magmas from common basaltic sources. Contrib Mineral Petrol 148:635–661
Sun YS, Nafi Toksoz M, Pei SP, Zhao DP, Morgan FD, Rosca A (2008) S wave tomography of the crust and uppermost mantle in China. J Geophys Res 113:B11307
Sun WD, Zhang H, Ling MX, Ding X, Chung SL, Zhou JB, Yang XL, Fan WM (2011) The genetic association of adakites and Cu-Au ore deposits. Int Geol Rev 53:691–703
Sun WD, Ling MX, Chung SL, Ding X, Yang XY, Liang HY, Fan WM, Goldfarb R, Yin QZ (2012a) Geochemical constraints on adakites of different origins and copper mineralization. J Geol 120:105–120
Sun WD, Ling MX, Ding X, Chung SL, Yang XY, Fan WM (2012b) The genetic association of adakites and Cu-Au ore deposits: a reply. Int Geol Rev 54:370–372
Tapponnier P, Lacassin R, Leloup PH, Scharer U, Zhong DA, Wu HW, Liu XH, Ji SC, Zhang LH, Zhong JY (1990) The Ailao Shan/Red River metamorphic belt: tertiary left-lateral shear between Indochina and South China. Nature 343:431–437
Thieblemont D, Stein G, Lescuyer JL (1997) Epithermal and porphyry deposits: the adakite connection. Comptes Rendus De L Academie Des Sciences Serie Ii Fascicule a-Sciences De La Terre Et Des Planets 325:103–109
Tran MD, Liu JL, Nguyen QL, Chen Y, Tang Y, Song ZJ, Zhang ZC, Zhao ZD (2014) Cenozoic high-K alkaline magmatism and associated Cu-Mo-Au mineralization in the Jinping-Fan Si Pan region, southeastern Ailao Shan-Red River shear zone, southwestern China-northwestern Vietnam. J Asian Earth Sci 79:858–772
Turner S, Arnaud N, Liu J, Rogers N, Hawkesworth C, Harris N, Kelley S, Calsteren PV, Deng W (1996) Post-collision shoshonitic volcanism on the Tibetan Plateau: Implications for convective thinning of the Lithosphere and the source of ocean island basalts. J Petrol 37:45–71
Wang XF, Metcalfe I, Jian P, He LQ, Wang CS (2000) The Jinshajiang-Ailaoshan Suture zone, China: tectonostratigraphy, age and evolution. J Asian Earth Sci 18:675–690
Wang DH, Qu WJ, Li ZW, Ying HL, Chen YC (2004a) The age of porphyry Cu-Mo deposits in Jinshajiang-Red River belt: Re-Os dating. Sci China Ser D Earth Sci 34:345–349 (in Chinese)
Wang Q, Xu JF, Zhao ZH, Bao ZW, Xu W, Xiong XL (2004b) Cretaceous high-potassium, intrusive rocks in the Yueshan-Hongzhen area of East China: Adakites in an extensional tectonic regime within a continent. Geochem J 38:417–434
Wang Q, Xu JF, Jian P, Bao ZW, Zhao ZH, Li CF, Xiong XL, Ma JL (2006) Petrogenesis of adakitic porphyries in an extensional tectonic setting, Dexing, South China: implications for the genesis of porphyry copper mineralization. J Petrol 47:119–144
Wang QF, Deng J, Li C, Li GJ, Yu L, Qiao L (2014) The boundary between the Simao and Yangtze blocks and their locations in Gondwana and Rodinia: constraints from detrital and inherited zircons. Gondwana Res 26:438–448
Whitney DL, Evans BW (2010) Abbreviations for names of rock-forming minerals. Am Mineral 95:185–187
Wyllie PJ, Sekine T (1982) The formation of mantle phlogopite in subduction zone hybridization. Contrib Mineral Petrol 79:375–380
Xu JF, Shinjo R, Defant MJ, Wang Q, Rapp RP (2002) Origin of Mesozoic adakitic intrusive rocks in the Ningzhen area of east China: partial melting of delaminated lower continental crust? Geology 30:1111–1114
Xu SM, Mo XX, Zeng PS, Zhang WH, Zhao HB, Zhao HD (2006) Characteristics and origin of alkali-rich porphyries from Beiya in W. Yunnan. Geoscience 20:527–535 (in Chinese with English abstract)
Xu LL, Bi XW, Su WC, Qi YQ, Li L, Chen YW, Dong SH, Tang YY (2011) Geochemical characteristics and petrogenesis of the quartz syenite porphyry from Tongchang porphyry Cu (Mo-Au) deposit in Jinping County, Yunnan Province. Acta Petrol Sin 27:3109–3122 (in Chinese with English abstract)
Xu H, Cui YL, Zhou JX, Zhang MH, Rong HF, Jiang YG (2015) LA-ICP-MS zircon U-Pb ages and geological implications of Baofengsi alkaline porphyries, Binchuan city, Yunnan province, China. Acta Mineral Sin 35:457–462
Xue CD, Hou ZQ, Liu X, Yang ZM, Liu YQ, Hao BW (2008) Petrogenesis and metallogenesis of the Beiya gold-polymetallic ore district, northwestern Yunnan province, China: response to the Indo-Asian collisional processes. Acta Petrol Sin 24:457–472 (in Chinese with English abstract)
Yang KH (1998) A plate reconstruction of the eastern Tethyan orogen in southwestern China. In: Flower, M.FJ., Chung, S.-L., Lo, C.-H., Lee, T.-Y. (Eds.), Mantle dynamics and plate interactions in East Asia. Geodynamics Series, American Geophysical Union 27: 269–287
Zeng PS, Hou ZQ, Gao YF, Du AD (2006) The Himalayan Cu-Mo-Au mineralization in the eastern Indo-Asian collision zone: constraints from Re-Os dating of molybdenite. Geol Rev 52:72–84 (in Chinese with English abstract)
Zhao X, Mo XX, Yu XH, Lu BX, Zhang J (2003) Mineralogical characteristics and petrogenesis of deep-derived xenoliths in Cenozoic syenite porphyry in Liuhe, western Yunnan province. Earth Sci Front 10:93–104 (in Chinese with English abstract)
Zhao X, Yu XH, Mo XX, Zhang J, Lu BX (2004) Petrological and geochemical characteristics of Cenozoic alkali-rich porphyries and xenoliths hosted in western Yunnan Province. Geoscience 18:217–228 (in Chinese with English abstract)
Zhao JH, Zhou MF, Yan DP, Zheng JP, Li JW (2011) Reappraisal of the ages of Neoproterozoic strata in South China: no connection with the Grenvillian orogeny. Geology 39:299–302
Zhou MF, Yang DP, Kennedy AK, Li YQ, Ding J (2002) SHRIMP U-Pb zircon geochronological and geochemical evidence for Neoproterozoic arc-magmatism along the margin of the Yangtze block, South China. Earth Planet Sci Lett 196:51–67
Zhou MF, Ma YX, Yan DP, Xia XP, Zhao JH, Sun M (2006) The Yanbian terrane (southern Sichuan Province, SW China): a Neoproterozoic arc assemblage in the western margin of the Yangtze block. Precambrian Res 144:19–38
Zhu XP, Mo XX, White NC, Zhang B, Sun MX, Wang SX, Zhao SL, Yang Y (2013) Petrogenesis and metallogenic setting of the Habo porphyry Cu-(Mo-Au) deposit, Yunnan, China. J Asian Earth Sci 66:188–203